BRNO UNIVERSITY OF TECHNOLOGY
VYSOKÉ UČENÍ TECHNICKÉ V BRNĚ

FACULTY OF ELECTRICAL ENGINEERING AND COMMUNICATION
FAKULTA ELEKTROTECHNIKY A KOMUNIKAČNÍCH TECHNOLOGIÍ

DEPARTMENT OF PHYSICS
ÚSTAV FYZIKY

ALTERNATIVE METHODS FOR THE ANALYSIS OF STRUCTURAL CHANGES IN MUSCLE TISSUE

ALTERNATIVNÍ ZPŮSOBY ANALÝZY STRUKTURÁLNÍCH ZMĚN SVALOVÉ TKÁNĚ

SHORT VERSION OF DOCTORAL THESIS
ZKRÁCENÁ VERZE DIZERTAČNÍ PRÁCE

AUTHOR — Ing. PAVEL KASPAR
AUTOR PRÁCE

SUPERVISOR — prof. Ing. LUBOMÍR GRMELA, CSc.
ŠKOLITEL

BRNO 2017

Keywords

Biological tissue, absorption, scattering, Monte Carlo, optical anisotropy, transmission, reflection

Klíčová slova

Biologické tkáně, rozptyl, absorpce, Monte Carlo, optická anizotropie, transmise, odraz

Content

1. Introduction

Biological tissues are materials difficult to precisely describe and measure, yet very important to understand. From the building blocks of our own bodies to the food we eat, they permeate almost every area of our existence. This work is focused on the consumption part and the related quality control of meat specifically, as the importance of proper and healthy diet and quality cannot be underestimated.

Consumption of meat is widely spread all over the globe, and as such is an important part of human diet. This is the reason for close monitoring of quality and safety of such a resource by both manufacturers and consumers alike. This tendency increases even more with recorded incidents [1]. The more distance the product has to travel from the production to consumers, the greater the probability of the natural processes in the meat and the environmental influences will cause meat spoilage [2, 3]. For those reasons, among others, is important to be able to detect and evaluate the safety and freshness of meat before distribution and consumption.

One of the evaluated properties during quality control is meat tenderness, which can correlate to many possible factors, like age of the animal, or its species. A usual method of such evaluation is the Warner-Bratzler Shear Force, which can be performed by texture meters or compression devices [4]. Another property to note is the water holding capacity, an often discussed feature of the meat. The measurement procedure focuses at gauging the speed of fluid loss during aging, cooking or freezing [5]. This is, however, a destructive measurement technique, damaging the sample, and was later replaced by non-destructive approaches. One of the most noteworthy of these is Near Infrared Spectroscopy (NIRS), able to quantify characteristics of the meat and its chemical properties [6, 7, 8]. A downside to this method is NIR capturing data from a single point only, making it less usable for a classification of quality for the whole bulk muscle tissue. Another approach uses the fact, that the internal chemical processes are often accompanied by changes visible on the outside of the bulk, like change in color, texture, and odorous releases. Acquisition of such information can be used for the quality analysis as Hyperspectral Imaging (HSI) [9, 10]. A somewhat improved version, less demanding on the cost and the amount of data observed making it possible to use with real-time applications, has risen in the form of Multispectral Imaging (MSI) [11, 12, 13]. These methods were also followed by several improvements to their efficiency, like the enhancement of the MSI algorithm for near-infrared wavelengths [14], or specific detection targeting of total volatile basic nitrogen content as one

of the important indicators of pork freshness [15]. Another property of the meat to be closely monitored is pH, which changes in correlation with natural decay of the tissue [16]. One of the more recent methods is based on measuring meat freshness by using light scattering inside of the bulk meat, while considering the specific internal structure of the sample, like collagen content and sarcomere lengths [17]. This interaction of light with the anatomical structure of the meat also inspired parts of this work.

As modern methods focus more and more on specific parameters of their measured objects, they often forgo the relationship between each of the changing parameters and the structural reason for these changes. The deeper they go the more complex and expensive the method becomes. In this dissertation a different kind of approach to the measurement of optical parameters and their practical use is described. Because biological tissue is such a complex material, every shift that happens is preceded and followed by a score of other changes. This not only makes the biological materials difficult to describe, it also brings the option of seeing these processes not as a discrete events to be characterized one by one, but by fusing the older approach of describing larger amounts of properties as one with modern knowledge and accessible technology we can address specific transformations of the inner structure. The focus has been placed on the changes in absorption scattering, polarization, refractive index and optical anisotropy of muscle tissue. As all of the methods described below require destructive approach to sampling and measurement in their current form, they are unfit to be used in medicine, and were used to characterize changes in porcine meat due to the decay over time and the exposure to the elements, such as drying and freezing. These processes are known to produce some structural changes. Therefore the goal was not to prove their existence, but rather to gain an understanding of the structural and chemical changes in the muscle tissue due to the alterations listed above, and to create methods and approaches that would allow the measurement of their changes without the use of complex measurement setups or expensive parts and instruments.

2. Thesis objectives

In this thesis the object of study were biological materials, namely muscle tissue. The whole process of working with such materials is usually very difficult, because it is necessary to combine knowledge from physics and biology, two very different fields. Two choices were made early on into the process: focus would be placed upon optical properties and the measurement would be performed and methods would be proposed for meat intended for consumption. These decisions were made because it was necessary to have a large pool of possible samples and to strive towards a real application.

The main objectives of the thesis were:

- Propose new and innovative methods of muscle tissue degradation analysis.
- Identify and focus on specific types of degradation and the usefulness of their detection in practical applications.

To achieve them another set of side goals had to be completed first and throughout the whole undertaking of the dissertation thesis:

- Research currently used methods of muscle tissue analysis and select a less explored direction.
- Understand the structure of muscle tissue and biological tissues altogether.
- Analyze the options and choose the suitable way of sampling.
- Get a basic grasp of chemical processes inside of the muscle tissue post mortem.
- Learn to create models of photon propagation through biological tissue and prepare such a model.

3. Sample preparation

Fresh samples of the day were transported for 30 minutes into the laboratory under refrigeration and then underwent immediate cutting and initial measurement. Samples of varying thickness were cut from each of the purchased bulk, to minimize the influence of sampling location and maximize the variety of the sample size. For the best sample quality those without any inclusions and the least amount of fat or ligament were prioritized. The cutting process was performed manually with a scalpel and the resulting samples were sorted by thickness with a tolerance of 0.1 mm and cutting angle with tolerance of 5° at the measured area. The samples not up to the standard were used in measurements to determine the influence of outside lighting on the measurement, the safety of the laser towards the muscle tissue in regards to photobleaching effect, and other calibration tasks, sorted by the nature and degree of the imperfections. This allowed the live procedures to be done with minimum waste and errors due to reworking of the methods. Even though the cutting was done manually, it required a lot of focus and repetition, and thus it is recommended to use a microtome for uniform and smooth cuts.

Samples subjected to natural aging outside a container were kept uncovered on a glass base slide away from direct light in room temperature of 21 °C and humidity of 45 %. Samples meant for freezing were sealed in plastic bags and cooled to the temperature of -18 °C. Drying was performed in an air of low humidity, around 30 %, and temperature of 50 °C for 6 hours, suspended in the air by hanging from one side so that the area designated for measurement would not come into contact with any object. Where smoking was performed, it was done on oak wood in a dry smoker at the temperature of around 95 °C for 8 hours. In the case of sample salting a Prague Powder Pink was used with 93.75 % table salt and 6.25 % sodium nitrate.

4. Scattering & Absorption measurement in muscle tissue and Monte Carlo simulation

4.1. Measurement setup

In order to successfully detect and replicate changes of optical properties in biological tissue with the possibility of usage outside of the laboratory we used easily accessible components for the creation of the measurement setup.

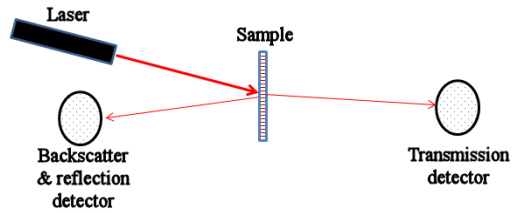

Figure 4.1. Schematic sketch of the scattering and absorption acquisition system.

As the illumination source a 5 mW He-Ne red laser was used. A CMOS digital camera for the photon spread detector and a Si switchable gain detector for ranges 350-1100 nm as the intensity sensor were selected. The digital camera was placed to detect the backscattered photons for majority of the measurements, but in some cases, where a recording of transmitted photons spread was required, it was relocated to the transmission detection location, a place usually occupied by the gain detector to measure absorption (Fig. 4.1.). Areas of both the camera and the gain detector remained same for the whole measurement, and the detector output was in the form of radiant flux expressed as voltage signal. As the method is based in comparing the results with the same measurement setup, rather than in specific numbers, the output obtained in voltage signal serves as relative value of the radiant flux detected. Detectors were placed in the distance of 5 cm from the sample to be as close as possible while still allowing manipulation of the components during measurement. In the process of measurement a conclusion was reached, that most of the scattering patterns required to be observed are more significant in the backscattered area, whereas the transmitted area provides better absorption readings (hence the usual configuration of detectors). The whole setup was encased in a box with light absorbing paint on the inside. This was done to prevent any light from the outside of reaching the detector and the escaped light to return back into the measurement. When comparison measurements were carried out, it was discovered that the resulting change was only in units of percent in the absence of black absorbing paint. In all likelihood the difference between keeping and eliminating the escaped light would be more visible in a tighter and more precise setup (for potential field use).

4.2. Illumination experiments

The samples for this measurement were cut from the long head of triceps brachii of a pig. The selected thickness was 5 mm in order to achieve acceptable information yield even with lower quality detection equipment. The samples were subjected to five types of alteration common to consumer meat: aging, drying, freezing, smoking and curing with salt. All of the samples were measured before and after alteration to allow the comparison of the results.

Selecting the angle of illumination was one of the first greater issues for detection in backscattered area. Reflected light tends to overpower the signal from backscattered light without the ability to discern between the two on the basis of their energy. For this measurement we do not require the reflected light, and an alternative was therefore chosen: a non-perpendicular angle of illumination of 60 °. While the reflected light behaves mostly as expected, with some minor changes due to the roughness of the surface of the sample, and the reflected angle is more or less equal to the angle of illumination, the backscattered light tends to have the angle affected by the angle of the illuminated muscle fibers. This might be caused by the fact that the muscle fibers are able to function as optical fibers in a limited capacity [18]. Crossing boundaries between separate myofibrils and muscle fibers causes the propagation direction of a photon to gradually even out with the direction of the fibers. Since all of the samples used for this measurement were cut perpendicularly to their muscle fibers, the direction of backscattered light is bent towards the perpendicular, the more so the deeper into the sample the photon penetrated before backscattering (Fig. 4.2.). This phenomenon allows for easier separation of backscattered and reflected photons.

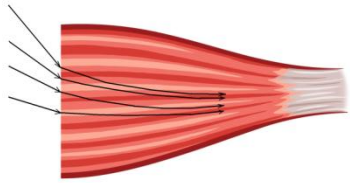

Figure 4.2. Photons entering the muscle cut across the fibers and evening out the course of their propagation to the direction of the fibers.

The properties chosen for observation were absorption, scattering, anisotropy and refraction. Reflection from the rough surface was deemed

to not carry the information we needed, especially because it tended to change with cutting techniques and the process itself, bringing in an unclassifiable variations between samples. Naturally there are more processes going on inside of the sample and each of the alterations the samples were subjected to result in a change in multiple observed optical properties, and some of the unobserved ones. By simplifying the observation only to the four properties it is possible to achieve meaningful results without falling victim to the pitfalls of attempting to precisely (and unduly complexly) describe the processes behind every alteration.

In order to match the simulation and the detected parameters of the measurement an artificial property of the scattering pattern was created, called the average area of impact. This was in its essence a simple elliptically shaped area, where the detected illumination would not drop under the threshold of 75 % of the maximum intensity value. Four different variables were then observed, that changed with the changes of optical properties. These were the center of the ellipse, sizes of the two axes of the ellipse (in regards to x and y coordinates), and the number of photons inside of the ellipse. This average area of impact was then used as a tool for analyzing the changes of the observed properties, since every property had a certain effect on the observed variables.

The first observed optical property was absorption due to the lack of complexity of the process. The decrease of detected light could be measured by detector in transmission. The simple act of intensity decrease is not enough to say the absorption has increased though, as the growth of a scattering pattern can also cause the ratio of photons incident on the sample and received on the gain detector to drop. Every observed property behaved in the same fashion, making the result only useful when viewed as a whole.

Changes in scattering were, on the other hand, the hardest to successfully evaluate. The concept of the scattering detection is fairly simply, as it consists only of detecting the change in the average area of impact: the smaller the area, the smaller the scattering. The problem comes again with the complementarity of the changes, as no alteration changes only a single property. The major issue is that basically any change within the sample will cause the shift in the size of the average area of impact, as it is affected by a number of possible internal processes. These are here substituted as a scattering. It is precisely for this reason that the decision to simplify the internal biological processes into the four optical properties was made.

The third observed optical property was the refractive index. The changes are reflected in the shift of the center of the average area of impact. The lower the refractive index of the tissue is, the further away the center of the average area of impact is to the point of impact of the laser on the sample, according to Snell's law (Fig. 4.3.). In muscle tissue there is also the effect of multiple scattering throughout the path of the photon through the sample. This can cause the angle of the transmitted photon to be different from the angle of the incident photon.

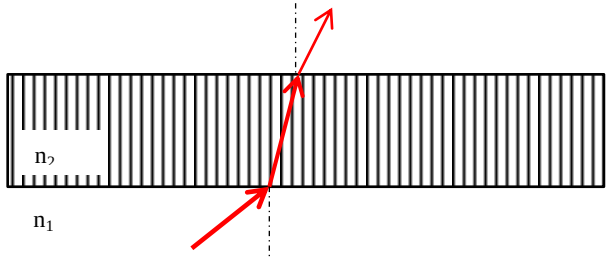

Figure 4.3. Propagation of light through refractive barriers with $n_2 > n_1$.

The last observed optical property was optical anisotropy. If the anisotropy changes at any point during the process, the result will manifest as a shift in the shape of the average area of impact. Since it is mathematically an ellipse, it can show the degree of anisotropy. When the sample is almost or entirely optically isotropic and the angle of impact is perpendicular, the average area of impact is circular. When the anisotropy starts to grow, the shape becomes more and more elliptical on one of its axes. This change is also visible when the angle of impact is oblique, but we have to take into account the fact that the original area of impact before alteration of the sample had some elliptical properties.

4.3. Monte Carlo simulation

Simulation of the photon propagation through the sample was created in MATLAB and based on a standard Monte Carlo algorithm [19, 20]. With enough changes, additions and enhancements the simulation is able to take into account not only the absorption and scattering coefficients, optical anisotropy of the sample and the optical indices of the medium and the sample, but the angle of incidence, changes in direction in cover slips, reflection on entry and exit and other minor factors as well. The precision calculations were run with up to 1 000 000 photons. As with the observed properties in the experimental part the main input and output data of the simulation are absorption and scattering coefficients, optical anisotropy and refractive indices of the materials. A result of a

simulation of an unaltered sample with detection in the backscattered area can be seen on Fig. 4.4, top, where the detector is considered to be 5 cm from the sample, the same as it is in the measurement setup. The average area of impact is located slightly to the left of the center of the axes, the 0,0 coordinates. That is also the location of the laser incidence on the sample. The scattering here is low, making the average area of impact to be tight and the low anisotropy provides for the lack of elliptical distortion. The reason for a lot of scattered photons being on the left side of the center is that in this case the illumination came from the left under the angle of 60 ° towards the sample and then the backscattered photons are bent to the direction of the fibers, thus causing them to be grouped towards the left side of the detector.

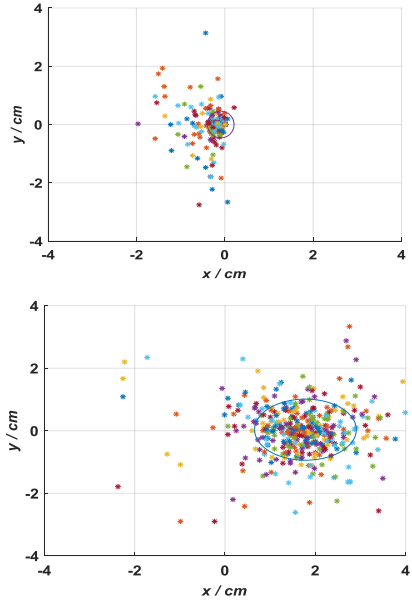

Figure 4.4. Average area of impact of photons of an unaltered sample on a backscattering detector (top) and the change in its shape, position and size due to sample alteration (bottom).

Since the measurement operates with average area of impact it is important to define it in the simulation as well. The center of the average area of impact is calculated as a two dimensional mean of the photon coordinates with standard deviations giving us the lengths of the two axes of the ellipse in the plane of impact on the detector. If the photons are more spread around one axes than the other, the center might not move but the shape of the ellipse will change.

The absolute values of the average area of impact from the experimental part and the simulation are not identical, but they were never expected to be. The most important part is that the changes they undergo are proportionally the same, therefore if one changes in any way, the other does as well by the same margin. Naturally this does not cover the amount of transmitted photons in the experimental part, but the intensity of the transmitted light changes proportionally with the amount of simulated photons as well.

The influence of changes in observed properties applies to the simulation as well. Changes in scattering will influence the size of the elliptical area of impact, the shift in anisotropy will cause one of the axes of the ellipse to be more or less pronounced and the change in refractive index will cause the center of the average area of impact to move. The result of all of these changes can be seen on an illustrative Fig. 4.4. bottom, in comparison to Fig. 4.4., top.

4.4. Heat Strain

This simulation can also be used to calculate the energy strain on the measured sample. It is highly important to prevent the degradation of the sample during the measurement by way of photobleaching (in this case heat degradation of the biological tissue). During photochemical effect, the energy of the illumination source can disrupt the chemical bonds on a molecular level, photothermal effects can increase the temperature of the sample and these can result into a cellular changes and damage. To prevent this from happening, and contaminating our results from measurement an optimal intensity of the laser should be used, while balancing the signal to noise ratio as well (increased intensity of the illumination source increases signal output, but also the noise generated by a variety of issues in the measurement [21]). A certain amount of energy is absorbed while the light travels through a tissue. This amount can be calculated from the average absorption value provided by the Monte Carlo simulation. To this end the energy of a single photon emitted by the laser must be calculated:

$$E = \frac{hc}{\lambda}, \tag{4.1}$$

where h is Planck constant (6,636 × 10^{-34} J.s), c is the speed of light (2,988 × 10^{8} m/s), and λ is the wavelength of the laser used (in our case 632 × 10^{-9} m).

The number of photons per second emitted by a laser of power P is given by:

$$n_q = P\lambda. \tag{4.2}$$

By finding the energy of the photon and the their number emitted per second we can then multiply the result by the average absorption in each of the simulation and gain the energy absorbed by the tissue. The ability of the tissue to dissipate the heat and transfer the energy also has to be taken into account, so the result of the energy strain calculation has to be adjusted by these values as well.

4.5. Results

Around 50 measurements were performed to provide us with information about the changes of the optical parameters due to the sample alterations. After the samples were measured estimations were made from a preexisting knowledge of biological processes [22, 23] about the changes in optical properties. These estimates were then used in the simulation and if the patterns were comparable with a difference of less than 10 %, the estimate was established as correct and from these, Table 1 was created.

Table 1. Changes in observed optical properties after altering the samples in comparison to their fresh state. 1 … a change was detected, 0 … no change was detected.

	Absorption	Refractive index	Scattering	Optical anisotropy
Aging	1	0	1	1
Drying	1	1	1	1
Freezing	1	0	0	1
Smoking	1	1	1	0
Curing	1	0	1	0

The change in absorption present during every alteration is most likely due to water loss that is unavoidable during any manipulation and aging of the sample but cannot be simply excluded from the observation, because the change in the amount of permitted photons can also be caused by shifts in scattering far away from the detection area. The magnitude of the absorption change also differs. It is also important to note that different types of muscle and different sampling locations might yield different table results because of the complicated structure and the non-homogeneity of the material. For example greater inclusion of lipid content or cartilage could affect the water volume in the tissue in a major way, thus giving different importance to the drying during alterations. If this method were to be used in the field, a proper calibration would have to be performed for specific species, muscle group and sampling location.

After the calibration a measurement of 30 blind samples was performed. The detected changes and simulated results were then compared to Table 1. From this set the identification of 23 samples was correct. 2 of the incorrect results were due to procedure error during the evaluation process and 5 were misidentified because the alteration was below the detectable threshold (not losing enough water during drying, aging only one day and so on). By this measurement it was possible to identify a refrozen sample, aging of 5 or more days and losing at least 50 % of the initial amount of water from the tissue.

5. Angular absorption of light in muscle tissue

5.1. Measurement setup

From the four observed optical properties in the previous chapter one of them did not get as much attention as it deserved. Absorption of light can be used in various scenarios to provide interesting information. Coupled with the inhomogeneity, non-linearity and anisotropy of biological tissue, every angle and situation should have different absorptive properties. One of the only stable structures in muscle tissue is the muscle fibers. Not only are they always present, but their basic structure remains the same. Of interest are primarily the structure of muscle fiber and the sarcolemma covering it.

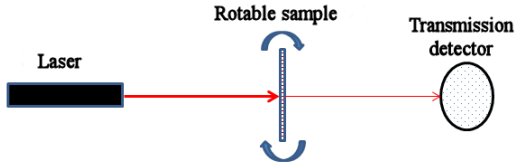

Figure 5.1. Schematic sketch of the angular absorption acquisition system.

To measure the absorption a simple system for light absorption in transmission was created (Fig. 5.1.). The illumination source is a 5 mW He-Ne laser with wavelength of λ = 632.8 nm with a collimated beam diameter of 2 mm. For holding the sample a table with the ability to rotate was used to allow different angles of illumination. The detector is a switchable Si detector with the detection range from 350 to 1100 nm with a voltage signal output for the transmitted radiant flux measurement. Area of the gain detector remained same for the whole measurement. As the method is based in comparing the results with the same measurement setup, rather than in specific numbers, the output obtained in voltage signal serves as relative value of the radiant flux detected. The goal is also not to establish specific database for the sample groups, but rather to provide the relative comparison of values from samples before and after the change. The distance between the source and the sample was set at 10 cm for computation simplification purposes. The distance between sample and detector was 5 cm to be as close as possible while allowing the table to freely rotate without coming into contact with the detector. The whole acquisition system was enclosed in a container with light absorbing paint on the inside to prevent outside and inside reflected illumination from entering the detector.

5.2. Sample groups measurement

Samples were cut from thirty bulks of fresh pork obtained on different days. Cuts were of different thickness to achieve minimal influence of sampling location and maximize the variety of the sample sizes. For the sampling purposes locations with the least amount of fat and ligament inclusions were prioritized. The purchase, cutting and first measurement were done in ten different days over the course of two months to avoid any bias in the tissue due to the meat source. The samples were then split into three groups with different values of thickness each numbering ten samples from ten different bulks (300 samples in total). The three main

groups differed by cutting angle of the muscle fibers in order to illustrate the influence of the angle on the light absorption. The cutting angles were 77 °, 103 ° and 120 ° to the direction of muscle fibers. Because every thickness of every cutting angle was measured on 10 different samples, the results were averaged to provide a single number for each angle of each thickness of the samples. The cutting process is important to the success of the measurement and it is therefore especially important for the cuts to be precise. The results of cutting are especially visible at thinner samples, where the cutting is one of the most challenging processes this method requires. It is also important to position the samples in such a way that minimizes decrease in light intensity of the transmitted light due to polarization [24] and preserving the setup for all of the measurements to ensure the same conditions for repeatability. The first group was subjected to aging, the second to freezing and the third group to drying.

Every sample was measured before any alteration on the day of the first unaltered measurement to provide the initial values of the fresh material that can be related to in further stages of the process, as seen in Figs. 5.2., 5.3. and 5.4. The difference in cutting angle in the three groups resulted in a shift of the absorption minimum while still adhering to the same profile between the various thicknesses. The cutting angle is marked with a black line on the x axis in the figures. According to expectations the least amount of absorption was detected in the angle of the muscle fibers, while the highest absorption was in the angle farthest away from the muscle fiber direction. This angular absorption profile combines not only the ability of the light to pass along the muscle fibers more easily, as it would in optical fibers, but also the increasing thickness of the sample in the way of photons in more oblique angles. Were the thickness due to angle of illumination the only source of absorption increase, the resulting angular profile would take normal distribution with the extreme in the middle. The position of the extremes and the shape of the profile clearly shows that the direction of the muscle fibers have greater influence than the increase in tissue thickness on fringe angles [25].

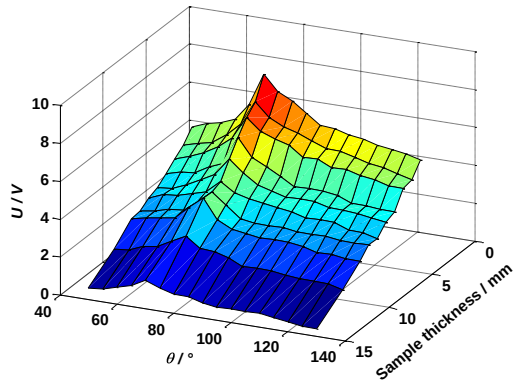

Figure 5.2. Angular distribution of light transmitted through the first group of fresh samples of different thickness. Light signal is converted into voltage on the detector. Cutting angle of 77 °.

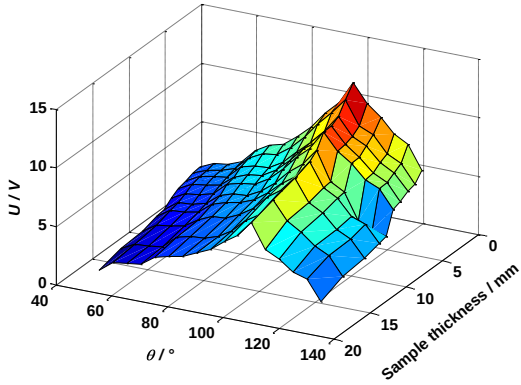

Figure 5.3. Angular distribution of light transmitted through the first group of fresh samples of different thickness. Light signal is converted into voltage on the detector. Cutting angle of 103 °.

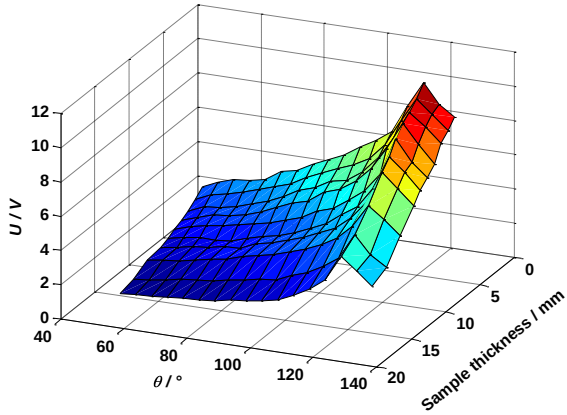

Figure 5.4. Angular distribution of light transmitted through the first group of fresh samples of different thickness. Light signal is converted into voltage on the detector. Cutting angle of 120 °.

The values recorded here are the means of 10 measurements from different samples each, a standard error for the means was also calculated. The values of the first measurements of the fresh samples can be seen in Table 2. During the sample alteration the values of standard errors varied only in the hundredths in comparison to the standard errors of the fresh states and are therefore omitted. The standard error percentages were much lower than expected and could be the result of the precision of selection and cutting process. While performing a measurement on the samples that did not pass the quality checks, the standard errors were 10 times higher. As it is reasonable to assume lower quality of samples during in situ measurements, it is highly recommended to not make samples thicker than 5 mm in accordance with the mentioned measurements.

Table 2. Percentage values of maximum and minimum standard errors of the means from 10 samples for each of the thickness and each group. Maximum and minimum values of SE were chosen from the measurement of angular dependency of absorption.

	Aging		Drying		Freezing	
Thickness / mm	Min / %	Max / %	Min / %	Max / %	Min / %	Max / %
3	0.15	0.24	-	-	-	-
4	0.33	0.31	0.10	0.48	0.21	0.46
5	0.25	0.31	0.14	0.53	0.12	0.51
6	0.36	0.51	0.17	0.46	0.14	0.69
7	0.38	0.53	0.13	0.62	0.17	0.99
8	0.48	0.58	0.17	0.71	0.28	1.67
9	0.50	0.54	0.14	0.99	0.38	2.08
10	0.64	0.97	0.31	1.89	0.41	2.41
12	0.99	1.44	0.29	1.98	0.58	2.88
14	-	-	-	-	0.63	5.69
15	2.50	5.32	0.42	2.99	-	-
16	-	-	-	-	1.08	8.24
18	-	-	0.62	5.19	-	-

The changes in the meat during aging (see chapter 5.3.1) cause an increase in absorption at the angle of maximum transmission, increasingly so with the time of aging. Where the differences between angles of maximum and minimum transmission were clearly visible in the fresh state (Figs. 5.2., 5.3. and 5.4.), during aging this difference starts to drop, and after 120 hours the reduction in difference in comparison to the fresh state approaches one third of the original value, as seen in Fig. 5.5.

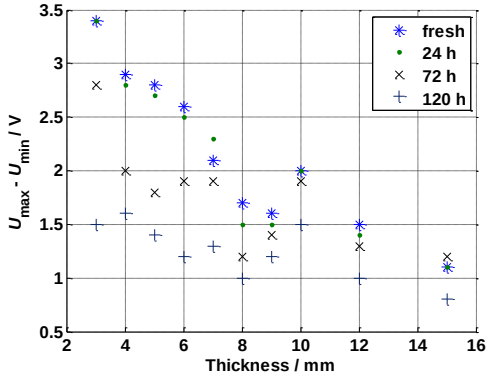

Figure 5.5. The difference between maximum and minimum absorption in dependency on the thickness of the sample and aging time.

During drying of the samples the water loss is the most prominent change in the tissue, much higher than during the aging procedure. Other changes together with the water loss cause the difference in the angular dependency of absorption to decrease, as seen in Table 3.

Angular dependency of absorption changes very little after the first round of freezing and thawing procedures, because the structural changes are not yet as pronounced as they are after second freezing and thawing procedure. The second freezing destroys even more of the internal structure of the meat sample, causing the minimum absorption value to increase (Fig. 5.6.) due to the distortion of the fibers, and the maximum absorption to decrease due to thinning of the structures in the tissue, providing us with the ability to differentiate the results from aging and drying, where the maximum and the minimum absorption both increased (Table 4).

Table 3. Measured percentage difference of absorption in samples compared to their fresh states during aging and drying, measured at minimum absorption angle.

	Aging			Drying
Thickness / mm	24 h / %	72 h / %	120 h / %	Dried / %
3	1.2	9.6	32.5	-
4	4.2	16.7	29.2	27.3
5	3.0	17.9	29.9	24.8
6	3.3	15.0	31.7	21.4
7	0.0	9.6	25.0	25.0
8	4.5	13.6	22.7	29.0
9	4.8	11.9	21.4	26.0
10	2.4	11.9	23.8	29.7
12	3.4	13.8	27.6	34.9
15	6.7	13.3	40.0	35.8
18	-	-	-	34.7

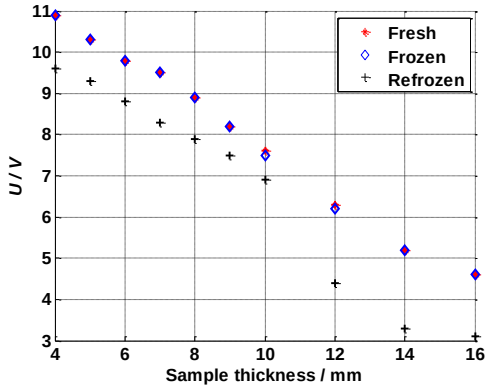

Figure 5.6. Changes in the amount of detected transmitted light converted into voltage on the detector during freezing, measured at minimum absorption angle.

Table 4. Measured percentage difference of absorption in samples compared to their fresh state during aging, drying and freezing, measured at maximum absorption angle (positive numbers stand for increase, negative for decrease).

	Aging			Drying	Freezing	
Thickness / mm	24 h / %	72 h / %	120 h / %	Dried / %	Frozen / %	Refrozen / %
3	2.0	4.1	16.3	-	-	-
4	4.7	7.0	18.6	8.8	0.0	-10.3
5	2.6	5.1	15.4	12.1	0.0	-4.0
6	2.9	5.9	14.7	12.9	0.0	-9.5
7	6.5	9.7	16.1	10.3	0.0	-10.5
8	0.0	3.7	11.1	8.0	0.0	-11.8
9	3.8	11.5	19.2	15.0	-6.7	-20.0
10	4.8	18.2	22.7	16.7	-7.7	-23.1
12	0.0	14.3	21.4	13.3	0.0	-8.3
14	-	-	-	-	0.0	-28.6
15	25	75.0	75.0	30.8	-	-
16	-	-	-	-	0.0	-40.0
18	-	-	-	50.0	-	-

5.3. Method efficiency

To find out the efficiency of the method a Wilcoxon signed-rank test was used to provide us with statistical analysis option for the differences between measurements of the samples in their fresh and altered states. Values of angular absorption from the measurements of each sample were tested against results of the same measurement angles after the alteration procedures. Table 5 illustrates the resulting findings. Changes during the aging process are recognizable from 72 hours onward, most of them even at the drying time of 24 hours. Drying of the tissue is also identifiable through this method, as seen in Table 5. For freezing and refreezing recognition process a more complex approach has to be taken, since testing the means of their absorption and transmittance yields no positive results. The change in overall absorption during freezing procedures was not proven to be significant, but the Table 4 shows that

the changes we need to pay attention to are at the angles with highest absorption, that is the furthest away from the cutting angle of the muscle fibers. At these angles the observed absorption increases, whereas closer to the cutting angle the absorption decreases, as with other alterations, thus causing the zero hypothesis of the test to not be disproven. For a successful recognition of refreezing a sample should be cut with an angle more oblique to the direction of the muscle fibers to allow not only the measurement in the angle if minimum absorption, but also at the angle of maximum absorption, where the changes from refreezing are most visible.

Table 5. p values of Wilcoxon signed-rank test for the mean values of transmitted signal for all three test groups, each type of alteration tested against their fresh state. The changes are significant if $p > 0.05$.

	Aging			Drying	Freezing	
Thickness / mm	24 h / p	72 h / p	120 h / p	Dried / p	Frozen / p	Refrozen / p
3	0.108	0.001	0.001	-	-	-
4	0.008	0.001	0.001	0.001	0.180	0.047
5	0.345	0.002	0.001	0.001	1.000	0.210
6	0.018	0.001	0.001	0.001	0.180	0.619
7	0.018	0.001	0.001	0.001	0.144	0.394
8	0.028	0.001	0.001	0.001	0.001	0.334
9	0.003	0.001	0.001	0.002	0.109	0.850
10	0.012	0.001	0.001	0.001	0.593	0.717
12	0.028	0.001	0.001	0.001	0.068	0.001
14	-	-	-	-	0.109	0.016
15	0.028	0.001	0.001	0.001	-	-
16	-	-	-	-	0.179	0.756
18	-	-	-	0.001	-	-

6. Shifts in polarization

6.1. Measurement setup

Light passing through a biological sample often shows signs of polarization depending on the orientation and the material of the tissue [26]. It is therefore important to subject this property of the biological tissue to tests and evaluations. There have been several studies on using linearly polarized light to attempt to analyze with mixed results [24, 27]. In this approach circularly polarized light was used. The reasons for this decision are twofold: to reduce the effect the angle of the muscle fibers has on the linearly polarized light, where there can be great discrepancies between the absorption of light polarized in the same axis as the muscle fibers are, and to increase the sensitivity of the method, because depolarization of circularly polarized light happens in a different manner and can therefore provide different information than in the case of linear polarization.

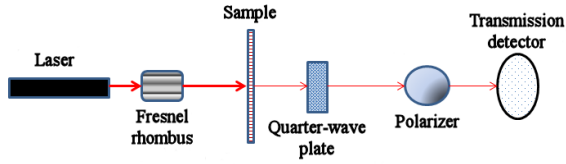

Figure 6.1. Schematic sketch of the polarization shift acquisition system.

For the illumination a 5 mW He-Ne red laser with wavelength of λ = 633 nm was used, as with the previous two methods. As laser is linearly polarized light, a conversion to circular polarization had to be introduced. To that end a Fresnel rhombus was used. For the measurement of Stokes parameter a zero order quarter-wave plate for the specific wavelength of λ = 633 nm was utilized. As an analyzer a polarizer with changeable angles was used. The detection was done by a switchable Si gain detector with the detection range from 350 to 1100 nm with a voltage signal output of the measured radiant flux (Fig. 6.1.). Area of the gain detector remained same for the whole measurement. As the method is based in comparing the results with the same measurement setup, rather than in specific numbers, the output obtained in voltage signal serves as relative value of the radiant flux detected. The distance between each of the optical components of the measurement setup was set at 5 cm for the shortest possible distance while still allowing for some manipulation of the components.

6.1. Polaization measurement

Samples were cut manually across the muscle fibers to allow the light to travel along the fibers during the experiment. Samples were then separated into three groups for further alteration by aging, freezing and drying. For the measurement itself, each of the three groups counted 5 samples of the same thickness, taken from 50 different bulks, every bulk providing one sample for each group to eliminate any bias caused by sampling sources.

From the measurement, where the Stokes parameters were the main focus, the dependency of degree of polarization (DOP) was gained. As can be seen in Fig. 6.2. DOP drops with the increasing thickness of the sample. Thicker samples than 5 mm were not measured due to the absorbance loss of the signal. To compensate for this loss it would be necessary to increase the power of the laser, but that would cause destruction of the sample due to photobleaching effect. In order to diminish the bias caused by inter-sample variability, each presented value is in fact average of the value of 5 samples of the same thickness and stage of alteration.

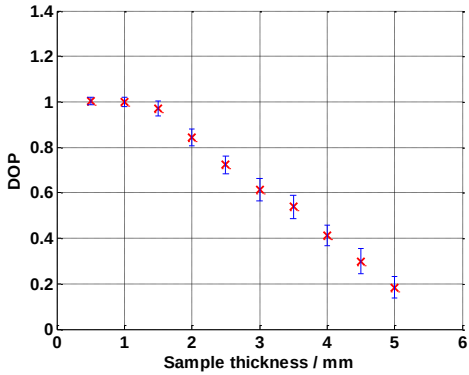

Figure 6.2. Thickness dependent average degree of polarization from fresh samples with standard errors.

The inter-sample variance of the measured values was also analyzed. From the Fig. 6.2. depicting average DOPs together with their standard errors it is visible that the variability spread of the values does influence the specific numbers, but does not influence the overall trend of the results. Standard errors were measured after sample alterations as well,

but their variance to the original value never exceeded 5 %. To avoid overloading the figures with needless data the standard errors are not depicted on other graphs, as they remained virtually unchanged and their presence does not improve the informational value.

Aside from degree of polarization *P* another two values were calculated for each set of Stokes parameters: degree of linear polarization P_L (DOLP) and degree of circular polarization P_C (DOCP):

$$P = \frac{\overline{S_1^2+S_2^2+S_3^2}}{S_0},$$
$$P_L = \frac{\overline{S_1^2+S_2^2}}{S_0}, \tag{6.1}$$
$$P_C = \frac{S_3}{S_0}.$$

Even though these values were calculated for every sample and measurement, the evaluation of aging is mostly performed on DOP only. To illustrate the reason for this the sample group with thickness of 1.5 mm was selected. The values are easier to observe in the thinner spectrum of the sample thicknesses used. As we can see in Table 6, DOLP very closely copies DOP, and is therefore redundant for this purpose. DOCP decreases very early in the aging process, and while this could be important information in its nature, it is not useful in the possible application because of the very short period in which it is distinguishable. The values of Stokes parameters on their own are also not particularly descriptive, though it is possible to judge the change in optical absorption during aging from the parameters S_0. Figure 6.3 shows the changes of DOP written in Table 6 for better illustration.

Table 6. Changes in Stokes parameters and various degrees of polarization from the 1.5 mm thick samples.

Time aged / h	0	2	4	8	12	24	48	72
S_0	72.8	66.8	58.1	50.0	42.1	38.1	32.0	30.5
S_1	0.2	0.4	0.3	1.4	0.5	0.9	0.6	1.3
S_2	70.7	49.9	40.3	28.4	17.8	13.4	9.0	8.0
S_3	0.3	0.7	0.6	0.2	0.1	0.1	0.1	0.0
DOP	0.97116	0.74710	0.69372	0.56870	0.42296	0.35208	0.28192	0.26573
DOLP	0.97115	0.74703	0.69365	0.56869	0.42297	0.35298	0.28187	0.26573
DOCP	0.00412	0.01048	0.01033	0.00400	0.00238	0.00262	0.00312	0.00001

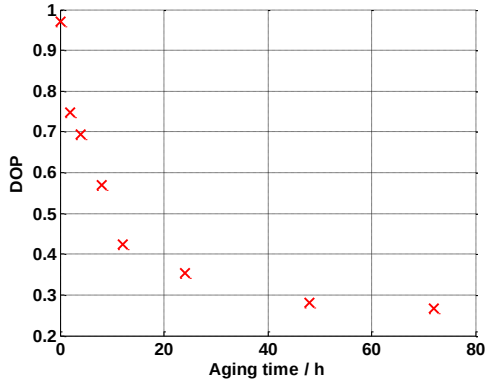

Figure 6.3. Degree of polarization changes during aging in samples of 1.5 mm thickness.

The second sample group was subjected to two courses of subsequent freezing with thawing and measurement after each course. As stated in chapter 5.3.3 about freezing and proven by the previous two methods in this thesis, the first course should not be easy to detect, while the second should show some differences. Such is the case in the polarization measurement as well. Table 7 shows the results of Stokes measurements of fresh sample and after first and second freezing in the example sample of thickness of 1.5 mm. The changes in Stokes parameters and the degrees of polarization from fresh to frozen sample are hardly discernible. The important shift occurs after the second course of freezing and thawing. While DOP and DOLP have only vary small variations to their fresh and once frozen versions, DOCP is where the important part lies. All Stokes parameters are increased in magnitude in different ratios. The increment on S_0, describing the rate of transmission, or rather the inverted value of absorption, corresponds with the measurement and results drawn from chapter 4 about angular absorption. The more important information for this method is, however, the major increase of DOCP of refrozen in comparison to once frozen samples.

Table 7. Stokes parameters and degrees of polarization of frozen and refrozen 1.5 mm thick samples

Alteration	fresh	frozen	refrozen
S0	72.8	71.9	78
S1	0.2	0.3	3.6
S2	70.7	69.7	74.5
S3	0.3	0.2	4.6
DOP	0.97117	0.96941	0.95806
DOLP	0.97116	0.96941	0.95624
DOCP	0.00412	0.00278	0.05897

Since the change in DOCP could be used to distinguish frozen from fresh meat while sampling from a bulk, the measurement was performed on the rest of the thicknesses of samples, which resulted in Fig. 6.4. The change in DOCP is clearly visible and both frozen and refrozen samples follow the same trend with increasing thickness. The drawback of the measurement is that the thicker the sample is, the smaller amount of photons is transmitted and therefore the signal yield drops. This also affects the standard error. Even though it seems to be increasing only slightly with the increasing sample thickness, the decreasing signal yield is at fault. The measurement results show percentage of standard error around 1 % on the sample 0.5 mm thick, while on the 5 mm thickness it is over 35 %.

A number of samples were subjected to more cycles of freezing and thawing in an attempt to establish a basic trend of polarization shifts. Regardless of thickness the absorption continued to decrease with every freezing cycle beyond the second one, but the decrease was only minor, up to 10 % of the previous value and growing smaller every cycle until around fifth cycle when the change was negligible. Degrees of polarization followed the same trend, increasing by a minor amount after every cycle as the tissue became more and more homogenized by destruction of the internal structure.

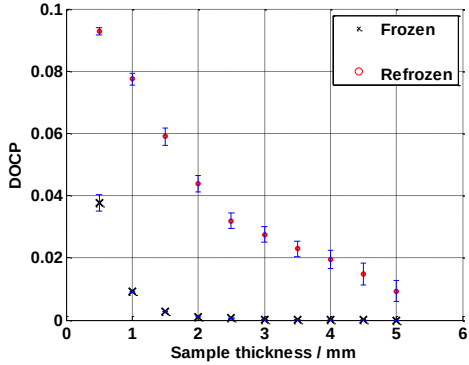

Figure 6.4. Changes in degree of circular polarization in the case of frozen and refrozen samples of varying thickness with standard errors included.

The third group, and the last alteration of the samples that was explored, was drying. In contrary to freezing the results of the drying process were below the ability of this method to distinguish between aged and dried material. Table 8 shows the comparison between aged samples and dried samples to illustrate their resemblance to one another and the difficulty of identification flowing from this similarity. As is clearly visible the dried results are virtually undistinguishable from the samples aged 48 hours.

Table 8. Stokes parameters and degrees of polarization for dried samples of 1.5 m thickness with values of the same category for fresh and aged samples for comparison.

Alteration	fresh	24 h	48 h	72 h	dried
S0	72.8	38.1	32.0	30.5	29.4
S1	0.2	0.9	0.6	1.3	1.6
S2	70.7	13.4	9.0	8.0	8.2
S3	0.3	0.1	0.1	0.0	0.1
DOP	0.97117	0.35251	0.28189	0.26574	0.28419
DOLP	0.97116	0.35250	0.28187	0.26574	0.28417
DOCP	0.00412	0.00262	0.00312	0.00001	0.00340

More types of drying other than the one specified in the chapter about sample preparation (Chapter 7.1) were attempted, with different air moisture, venting and temperatures, but the results were always similar to the aged measurement without any of the degrees of polarization stepping out of this line. The only observable change was that the absolute values of Stokes parameters were constantly lower than its aging counterparts. The relation between the Stokes parameters remained the same though, as is demonstrated by the various degrees of polarization. This difference in Stokes parameters did not follow any observable trend and registered large and irregular standard errors, making them virtually impossible to characterize in a descriptive and satisfying manner.

Conclusion

The presented thesis demonstrates three alternative methods for the optical analysis of structural changes in muscle tissue presented on samples of consumption pork. Very early on in the studying process it became clear that the greatest issue will be the nature of the material itself, since biological tissues in general are optically inhomogeneous, anisotropic and non-linear. This makes any attempt to diagnose any changes in them highly complicated. A great effort went into the development of the presented methods to find several functional approaches that are different from the established methods, while working with few and relatively basic instruments to create measurement setups that are innovate, yet accessible.

When compared to other established methods of in-depth physical analysis, like light scattering imaging techniques [17] or MSI [11] the required instruments for methods presented here are much simpler and an option of creating a portable version of the system is available, requiring a user with basic knowledge of anatomy and physiology of the sampled species. The sampling process with a lack of proper knowledge could prove an issue outside of laboratory conditions, because wrong selection of sampling location with high adipose or collagen tissue percentage would affect the results and likely prevent the attainment of correct results. With sufficiently efficient components the proposed approaches to analysis could be basis for an ideal field tool requiring much shorter time for sampling and processing and only a basic level of knowledge from the operator to prevent improper handling of the device or misinterpretation of the results.

While creating the scattering and absorption measurement a workable model of photon propagation through tissue was constructed. Together with the measurement itself a new and simple way of judging the photon scattering pattern was created in the form of the average area of impact. By using the average area of impact measurement of changes in the usually observed optical properties and photon-matter interactions induced by them, like absorption, scattering, reflection, refraction and anisotropy, is possible. By coupling measurement results together with the simulation it is possible to determine what groups of properties changed, though it serves to provide a general idea about what optical properties have changed rather than how much they differ. To successfully evaluate the results some previous empirical knowledge of the method and the measurements is required, as during the testing and calibration period the success of result categorization followed an increasing trend. Another downside of this approach is a relatively high

computational time, especially when the numbers of photons approach real values (millions or more). By improving the simulation and allowing it to reversely calculate the optical properties from existing measured average area of impact it should be possible to eliminate the estimation experience needed since the visual confirmation of results would not be necessary the time required to draw the results would be cut significantly.

The Angular absorption approach goes deeper in the detection of changes in radiant flux caused by sample alteration. Compared to the scattering and absorption method it has somewhat smaller detection span as far as types of alteration are concerned, but when focusing on freezing specifically it provides much better results. While this approach is also able to detect some changes between fresh and dried or fresh and aged meat samples, the biggest and the most visible difference is in the ability to discern between meat that is fresh and one that has undergone two cycles of freezing and thawing. The option to detect two cycles of freezing might prove invaluable to food quality control, even though one cycle of freezing shows virtually no changes, since the difference in meat being frozen once or twice is a huge one from both safety and consumption points of view. This is likely the biggest strength of the method. Details have also been published in an Impact Journal [25]. This method can, however, suffer by inconsistency in the sampling process. To improve the process and make it more accessible to inexperienced operators it would be necessary to create an easy to use sampling kit with instructions and illustrated sampling locations and techniques.

The third method focused on shifts in polarization between fresh and altered muscle tissue samples. Following the same sampling procedures as the two previously mentioned methods to have a common basis the measurement showed a certain redundancy in data for the whole 360 ° angular approach. The following adjustment to detection of Stokes parameters obtained from radiant flux measurement and subsequent calculation of degrees of polarization provided us with sufficiently distinct results. While it showed virtually no recognizable change between aging and dried sample, the difference between muscle tissue that was fresh, aged and one that underwent two cycles of freezing was clear. This outcome further supports the claims made in the section about angular absorption, that is the detectability of changes during subsequent freezing and thawing cycles via photon transmission measurement. The approach using the measurement of full range of 360 ° with the inclusion of Stokes parameter measurement would likely provide the same results in the observed areas, and some more potentially valuable data, but the measurement time required for each sample would be drastically

increased. The potential improvement of this method could, however, make use of this and attempt to incorporate the results of the angular dependency of the intensity of polarized light into the Stokes parameters for a chance of more relevant data and better sensitivity and specificity of the whole assessment technique.

All three proposed methods have two things in common. They are all laboratory-based and they all work with relative shifts in the observed optical properties. To make them portable and widely usable it would be necessary to create a special housing for the measurement setup, and mainly to assemble a database out of several hundreds of measured samples to create reference values and calibration standards for each measured muscle tissue origin species and sampling location. It would also be possible to combine the three proposed methods into one, because they share the sampling format, illumination source and some instruments. By cross referencing their results the precision of the resulting process would also be improved. By creating this combined device the presented methods could provide a tool for in-situ meat quality measurement and the detection and recognition of type of degradation the meat underwent.

References

[1] TRIENKENS, J., & ZUURBIER, P. Quality and safety standards in the food industry, development and challenges. *International Journal of Production Economics*. 2008, 113(1), 107-122. ISSN 0925-5273.

[2] NYCHAS, G.-J. E., SKANDAMIS, P. N., TASSOU, C. C., & KOUTSOUMANIS, K. P. Meat spoilage during distribution. *Meat Science.* 2008, 78(1-2), 77-89. ISSN 0309-1740.

[3] HUANG, L., ZHAO, J., CHEN, Q., & ZHANG, Y. Nondestructive measurement of total volatile basic nitrogen (TVB-N) in pork meat by integrating near infrared spectroscopy, computer vision and electronic nose techniques. *Food Chemistry.* 2014, 145(5), 228-236. ISSN 0308-8146.

[4] XIONG, Y. L., GOWER, M. J., LI, C., ELMORE, C. A., CROMWELL, G. L., & LINDEMANN, M. D. Effect of dietary ractopamine on tenderness and postmortem protein degradation of pork muscle. *Meat Science.* 2006, 73(4), 600-604. ISSN 0309-1740.

[5] TEJERINA, D., GARCÍA-TORRES, S., & CAVA, R. Water-holding capacity and instrumental texture properties of *M. longissimus* dorsi and *M. serratus* ventralis from iberian pigs as affected by the production system. *Livestock Science.* 2008, 148(1-2), 41-46. ISSN 1871-1413.

[6] PEDERSEN, D. K., MOREL, S., ANDERSEN, H. J., & BALLING, S. E. Early prediction of water holding capacity in meat by multivariate vibrational spectroscopy. *Meat Science.* 2003, 65(1), 581-592. ISSN 0309-1740.

[7] PREVOLNIK, M., ČANDEK-POTOKAR, M., & ŠKORJANC, D. Predicting pork water-holding capacity with NIR spectroscopy in relation to different reference methods. *Journal of Food Engineering.* 2010, 98, 347-352. ISSN 0260-8774.

[8] FOWLER, S. M., SCHMIDT, H., VAN DE VEN, R., WYNN, P., & HOPKINS, D. L. Raman spectroscopy copared against traditional predictors of shear force in lamb *M. longissimus* lumborum. *Meat Science.* 2014, 98(4), 652-656. ISSN 0309-1740.

[9] CLUFF, K., NAGANATHAN, G. K., SUGGIAH, J., SAMAL, A., & CALKINS, C. R. Optical scatering with hyperspectral imaging to to classify longissimus dorsi muscle based on beef tenderness using multivariate modeling. *Meat Science.* 2013, 95(1), 42-50. ISSN 0309-1740.

[10] ELMASRY, G., SUN, D. –W., & ALLEN, P. Near-infrared hyperspectral imaging for predicting colour, pH and tenderness

of fresh beef. *Journal of Food Engineering.* 2012, 110(1), 127-140. ISSN 0260-8774.

[11] LEVENSON, R. M., & MANSFIELD, J. R. Multispectral imaging in biology and medicine: Slices of life. *Cytometry.* 2006, 69(A), 748-758. ISSN 1552-4930.

[12] SUN. X., CHEN, K. J., MADDOCK-CARLIN, K. R., ANDERSON, V. L., LEPPER, A. N., SCHWARTZ, C. A., & BERG, E. P. Predicting beef tenderness using color and multispectral image texture features. *Meat Science.* 2012, 92(4), 386-393. ISSN 0309-1740.

[13] PANADOU, E. Z., PAPADOPOULOU, O., CARSTENSEN, J. M., & NYCHAS, G. –J. E. Potential of multispectral imaging technology for rapid non-destructive determination of the microbiological quality of beef filets during aerobic storage. *International Journal of Food Microbiology.* 2014, 177, 1-11. ISSN 0168-1605.

[14] HUANG, Q., LI, H., ZHAO, J., HUANG, G., & CHEN, Q. Non-destructively sensing pork quality using near infrared multispectral imaging technique. *Royal Society of Chemistry Advances.* 2015, 5, 95903-95910. ISSN 2046-2069.

[15] HUANG, Q., CHEN, Q., LI, H., HUANG, G., OUYANG, Q., & ZHAO, J. Non-destructively sensing pork's freshness indicator using near infrared multispectral imaging technique. *Journal of Food Engineering.* 2015, 154, 69-75. ISSN 0260-8774.

[16] DAMEZ, J. –L., CLERJON, S., ABOUELKARAM, S., & LEPETIT, J. Beef meat electrical impedance spectroscopy and anisotropy sensing for non-invasive early assessment of meat ageing. *Journal of Food Engineering.* 2008, 85, 116-122. ISSN 0260-8774.

[17] LI, H., SUN, X., PAN, W., KUTSANEDZIE, F., ZHAO, J., & CHEN, Q. Feasibility study on non-destructively sensing meat's freshness using light scattering imaging technique. *Meat Science.* 2016, 119, 102-109. ISSN 0309-1740.

[18] TEARNEY, G. J., BREZINSKI, M. E., SOUTHERN, J. F., BOUMA, B. E., HEE, M. R., & FUJIMOTO, J. G. Determination of the refractive index of highly scattering human tissue by optical coherence tomography. *Optic Letters.* 1995, 20(21), 2258-2260. ISSN 0146-9592.

[19] LANDAU, D. P., & BINDER, K. *A Guide to Monte Carlo Simulations in Statistical Physics.* Cambridge: Cambridge University Press, 2009. 3rd edition. ISBN 978-0-521-76848-1.

[20] PRAHL, S. A., KEIJZER, M., JACQUES, S. L., & WELCH, A. J. A Monte Carlo model of light propagation in tissue. In: *SPIE*

Proceedings of Dosimetry of Laser Radiation in Medicine and Biology. 1989, 102-111.
[21] Jan, J. *Číslicová filtrace, analýza a restaurace signálů.* Brno: VUTIUM, 2002. 2nd edition. ISBN 8021415584.
[22] HALL, J. E., & GUYTON, A. C. *Guyton and Hall Textbook of Medical Physiology.* Philadelphia: Saunders Elsevier, 2011. 12th edition. ISBN 978-1416045748.
[23] DUBOWITZ, V., SEWRY, C. A., & OLDFORS, A. *Muscle Biopsy: A Practical Approach.* Philadelphia, Saunder Elsevier, 2013. 4th edition. ISBN 9780702043406.
[24] JACQUES, S. L., ROMAN, J. R., & LEE, K. Imaging superficial tissues with polarized light. *Lasers in Surgery and Medicine.* 200, 26, 119-129. ISSN 1096-9101.
[25] KASPAR, P., PROKOPYEVA, E., TOMÁNEK, P., & GRMELA, L. Angular absorption of light used for evaluation of structural damage to porcine meat caused by aging, drying and freezing. *Meat Science.* 2017, 126, 22-28. ISSN 0309-1740.
[26] SANKARAN, V., EVERETT, M. J., MAITLAND, D. J., & WALSH, T. Comparison of polarized-light propagation in biological tissue and phantoms. *Optics Letters.* 1999, 24(15), 1044-1046. ISSN 0146-9592.
[27] GHOSH, N., WOOD, M. F. G., LI, S., WEISEL, R. D., WILSON, B. C., LI, R. –K., & VITKIN, I. A. Mueller matrix decomposition for polarized light assessment of biological tissues. *Journal of Biophotonics.* 2009, 2(3), 145-156. ISSN 1864-0648.

Selected author articles relating to the topic of dissertation

[A1] KASPAR, P., PROKOPYEVA, E., TOMÁNEK, P., & GRMELA, L. Angular absorption of light used for evaluation of structural damage to porcine meat caused by aging, drying and freezing. *Meat Science.* 2017, 126, 22-28. ISSN 0309-1740.

[A2] KASPAR, P., PROKOPYEVA, E., TOMÁNEK, P., & GRMELA, L. Changes in optical properties of biological tissue: experiment and Monte Carlo simulation. In: *Proceedings of SPIE 10142, 20th Slovak-Czech-Polish Optical Converence on Wave and Quantum Aspects of Contemporary Optics.* 2016.

[A3] KASPAR, P., PROKOPYEVA, E., TOMÁNEK, P., & GRMELA, L. Optical scattering in muscle tissue and its utilisation. In: *Proceedings of SPIE.* 2015, 9442, 20|1-20|7. ISSN 0277-786X.

[A4] KASPAR, P. Monte Carlo calculation of energy strain on a muscle fiber due to light absorption. In: *EEICT Proceedings of 21st Student Competition Conference.* 2015, 521-525. ISBN 9788021451483.

Professional CV

Ing. Pavel Kaspar
Faculty of Electrical Engineering and Communication
Brno University of Technology
Technická 8
616 00 Brno
E-mail: xkaspa25@stud.feec.vutbr.cz
Tel: +420 54114 6009

Education:
2013 – 2017: Doctoral study. "Physical Electronics and Nanotechnology"
2011 – 2013: Master. "Biomedical Engineering and Bioinformatics"
2008 – 2011: Bachelor. "Biomedical Technology and Bioinformatics"

Projects participation:
2017 – now: "Inovativní metody diagnostiky optických a elektronických vlastností organických a anorganických materiálů a struktur", FEKT-S-17-4626.
2014 – 2016: Rozvoj pokročilých metod pro diagnostiku elektrotechnických materiálů a součástek", FEKT-S-14-2240.

Employment history:
2016 – now: Department of Physics, Brno University of Technology, Czech Republic.
2013 – 2015: Central European Institute of Technology, Brno, Czech Republic.

Internships and professional practice:
Development of portable aerial carbon monoxide detector. Friedrich-Schiller University of Jena & IPHT Jena, Germany. 1. 2. – 31. 3. 2014.
Podzimní škola základů elektronové mikroskopie, Ústav přístrojové techniky AV ČR, v. v. i., Brno, 14-18. 10. 2013.
Electron microscopy, preparation of samples and measurement, Department of Histology and Embryology, Faculty of Medicine, Masaryk University, Brno. 1-31. 7. 2010 & 1-31. 7. 2012

Abstract

In this dissertation the topic of structural change analysis of muscle tissue and the methodical approach to this measurement is explored. Even though a considerable number of detection methods for the evaluation of specific changes in muscles exist, especially in the meat intended for consumption, the vast majority focuses only on a single process within the tissue and requires complicated approach and expensive instruments. The topic of this work is therefore not finding more precise and specific means of analysis, than the already existing ones, but rather to select an alternative approach to the given problematic. Part of the explored approach is also the endeavor to find a way to bypass the technological requirements while staying as close to the informational value of the high end methods as possible. To this end an informational base of theoretical knowledge and the experience in experimental approaches in the field of physics, optics and biological tissues and processes is required. The three main approaches described in this work are based on the acquired information throughout the research of the topic and understanding of the basic workings of muscle tissue.

The methods created for this thesis make use of photons in the transmission and reflection measurement setup. By observing the changes in absorption, dispersion and polarization of the light after the interaction with muscle tissue sample the other optical parameters are evaluated, including the refractive index and optical anisotropy. The identification of changes in optical parameters together with the Monte Carlo simulation allows for distinction between fresh, aged, dried, frozen and thawed, and refrozen and thawed samples.

Abstrakt

Tato disertační práce se zabývá tématikou analýzy strukturálních změn ve svalové tkáni a metodikou optického měření. I přesto, že existuje nezanedbatelné množství metod pro detekci konkrétních změn ve svalovině, především pak v konzumním mase, drtivá většina z nich se zaměřuje na jeden konkrétní proces a vyžaduje komplikované postupy a drahé přístroje. Předmětem prezentovaného výzkumu není tedy nalézt metody přesnější a specifičtější, než jsou ty již exitující, ale raději zvolit alternativní přístup k problematice. Součástí je pak i snaha najít možnosti jak obejít technologické nároky moderních postupů a přitom se přiblížit co nejvíce jejich informačnímu přínosu. Za tímto účelem je potřeba mít dostatečné teoretické znalosti a experimentální zkušenosti především v oboru fyziky, optiky a postupů měření, ale také široké povědomí o problematice biologických tkání a procesů v nich probíhajících. Na základě získaných informací a pochopení pochodů ve svalové tkáni jsou navrhnuty a testovány tři rozdílné přístupy.

Vytvořené metody pracují s fotony v transmisním i reflexním uspořádání. Pomocí pozorování změn absorpce, rozptylu a polarizace světla po interakci se vzorkem svalové tkáně jsou posouzeny jeho další optické vlastnosti především index lomu a optická anizotropie. Identifikace změn optických vlastností vzorků za různých podmínek umožňuje společně se simulací Monte Carlo posoudit rozdíly mezi vzorky čerstvými, starými, sušenými a jednou či dvakrát zmraženými a rozmraženými.